Studies and Analysis of the Impact of Part Orientation in Selective Laser Sintering Process on Mechanical and Structural Properties

Anna Floriańczyk, Roman Grygoruk, Marcin Bajkowski

Warsaw University of Technology
annam1309@gmail.com

Abstract

The aim of this study was to assess the results of experimental tests on the impact of orientation and location of the parts in the building room for the selective sintering of powders (SLS - Selective Laser Sintering), on the fundamental strength and structural parameters of specimens prepared according to DIN EN ISO 527, DIN EN ISO 178, DIN EN ISO 179, DIN 53505 and DIN 53736. The experimental results were further verified by SEM analysis and numerical simulations for specimens of sintered powder PA2200 polyamide. The research allowed to determine the correlation between the orientation and location of parts in the building room and the properties of the elements of polyamide powders as well as assess their impact on the quality of the sintered product.

Keywords: Selective Laser Sintering, SEM analysis, Rapid Prototyping, part orientation, polyamide powder, mechanical properties of materials

1. Introduction

Selective Laser Sintering (SLS) is a generative manufacturing technology already patented in the 80's and for years used to build material models, prototype elements and less for final products [Gibson I., et al. 2009, Meagan R., et al. 2011]. A material model, as in other rapid prototyping techniques, is based on a 3D geometric model stored in a proprietary format (e.g. STL). The beam of the laser sinters a layer - first the outline section, then fills the interior section of the layer. On the micro level, this means melting the outer layer of the particles, the core of which remains intact and combining with the outer layer of other particles [Jhabvala J. et al. 2013]. After hardening the working platform is lowered by the thickness of the layer and re-distribution of the powder occurs. The hardening process of the already sintered layer causes the next layer melting. This results in the formation of a solid model, which is supported by powder filling the building room [Meagan R., et al. 2011, Vandenbroucke B., et al., 2007].

Recently, we can see a trend toward using SLS technology in the final stages of producing short run final products. In this situation, demands on components manufactured in SLS technology concerning mechanical properties and surface quality are increasing continuously. It is particularly important to know the mechanical strength and maximal deformation of parts made in SLS technology in various envisaged load conditions. The temperature gradient distribution in the building room is characteristic in the sintering process [Mager A., et al. 2011, Parthasarathy J., et al., 2011]. Therefore it is essential to learn, like for FDM and SLA technologies, the impact of the orientation and location of the virtual models in the building room on the final geometrical, strength and structural properties of products [Singh R., 2013, Dąbrowska-Tkaczyk A., et al. 2011].

The issues of properties of elements made in rapid prototyping techniques (with numerous factors affecting them) as well as new applications have been undertaken by a number of research centres, mainly foreign ones**.** However, the majority of studies are mainly related to technology FDM (Fused Deposition Modelling) [Anitha R., et al. 2001, Wesley M., et al., 2013], and SLA (Stereolithography) [Cheng W., et al. 1995]. Studies on properties of components made in the SLS technology were conducted by, among others, [Usher, J.S. and Srinivasan, M.K., 2001]. They analysed the effect of laser sintering parameters (such as laser power) on the dimensional contoured accuracy of the elements produced (including horizontal, vertical and diagonal profiles of different sizes). However, their experimental studies did not consider the mechanical properties. On the other hand, other researchers, [Choren, J., et al. 2001] concerned only two parameters determining the mechanical properties (Ultimate Tensile Strength (UTS) and elastic modulus (E)) of elements made from the recovered powder in the recycling process. They studied only one value for each speed setting sintering, and the thickness of the layer. Tests on the degree of sintering of the particles (DPM) in the SLS have shown that increased DPM provides a higher tensile strength and higher elongation [Majewski et al., 2008]. Comprehensive research on the impact of sintering parameters (peak power density of the laser pulse, laser speed, laser power, sintered layer thickness) on the hardness, density and porosity of the sintered parts was conducted by [Dingal S., et al. 2008], however, test materials were iron powders.

A detailed study of specimens of nylon 12 arranged in different positions in the building room were conducted by [Usher J. S. et al., 2013], however, these studies focused on determining the relationship between the magnitude of the beam energy density, the setting portion and the tensile strength and elongation. The results of their research show that there is a correlation between the orientation of the part, the laser beam energy density and the mechanical properties of sintered powder of nylon 12 (for maximum elongation 15-16% the recommended value of beam's energy density is 0,25 Ws/mm^3, and for the maximum tensile strength of the order of 52MPa - the laser beam energy density of 0,40 Ws/mm^3, the worst mechanical

properties, regardless of the setting parameters of the laser gives the position ZX) [Dingal S., et al. 2008].

The researches of this kind, on the impact of selected parameters of the sintering process on mechanical properties, are more numerous [Zarringhalam, H., et al., 2006, Ajoku U., et al., 2006, Caulfield b., et al., 2007, Ramos - Grez J., et al., 2008], however, there are no comprehensive research results for thermo-mechanical properties in conjunction with the orientation and location of elements in the building room of the device.

Another comprehensive studies of mechanical, thermal and structural properties of the components made with rapid prototyping method will allow to verify the applicability of these materials in the construction of machine elements, special objects and biomedical engineering.

2. Material and methods

The aim of the study were comprehensive tests of specimens sintered polyamide 12 powder, placed in the building room in the vertical position, the horizontal position and on the edge for two positions: near the wall of the chamber (B) and in its centre (S). This meant: 8 combinations for uniaxial tensile tests (UTS), 8 combinations for bending tests, 6 combinations for Charpy impact tests, 6 combinations for thermal tests, and 6 combination for hardness tests.

3D-geometrical models of specimens were prepared (in SolidWorks®) according to the relevant standards [DIN EN ISO 527, DIN EN ISO 178, DIN EN ISO 179, DIN 53505, DIN 53736] in SolidWorks (Table 1).

Specimens (Table 1) were made on Formiga P100 using PA 2200. It is a fine-powder on the basis of polyamide 12. In comparison to standard polyamide 12, PA2200 is characterized by higher cristallinity and higher melting point as a result of specific production process. PA2200 contains stabilizers against heat and oxidation [Standards: DIN EN ISO 53736]. In the technological process the following parameters were applied: layer thickness - 0.1 mm, scan spacing - 0,1mm, laser power - 9W, laser speed -3500mm/sec. Certain mechanical and thermal properties of sintered powder are shown in Table 2.

Table 1. Geometrical dimensions of specimens for mechanical and thermal tests

Specimen's dimensions by DIN standards	Virtual model 3D-CAD
Unaxial Tensile Test (DIN EN ISO 527):	
Bend Test (DIN EN ISO 178):	
Charpy Impact Test (DIN EN ISO 179)	
Thermal Test (DIN 53736):	
Shore-D-Hardness Test (DIN 53505):	

Table 2. Some thermo-mechanical properties of sintered polyamide powder PA2200

Parameter	Value
Tensile modulus	1700 ± 150 N/mm^2
Tensile strength	45 ± 3 N/mm^2
Elongation at break	$20\pm5\%$
Flexural modulus	1240 ± 130 N/mm^2
Charpy-Impact strength	$53\pm3,8$ kJ/m^2
Charpy-Notched impact strength	$4,8\pm0,3$ kJ/m^2
Shore-D-hardness	$77,6\pm2$
Softening temperature	172-180°C

Then in Magics® the specimens were located in a virtual space of Formiga's building room according to the markings (Fig. 1b):

- for uniaxial tensile tests (UTS): vertically and in the middle of the building room (S_20_4), vertically and near the wall of the building room (B_20_4), horizontally and in the middle of the building room (S_150_20), horizontally and near the wall of the building room (B_150_20), on flank and in the middle of the building room (S_150_4), on flank and near the wall of the building room (B_150_4), on the edge and in the middle of the building room (S_edge), on the edge and near the wall of the building room (B_edge);

- for bend tests: vertically and in the middle of the building room (S_10_4), vertically and near the wall of the building room (B_10_4), horizontally and in the middle of the building room (S_80_10), horizontally and near the wall of the building room (B_80_10), on flank and in the middle of the building room (S_80_4), on flank and near the wall of the building room (B_80_4), on the edge and in the middle of the building room (S_edge), on the edge and near the wall of the building room (B_edge);

- for Charpy impact tests: vertically and in the middle of the building room (S_10_10), vertically and near the wall of the building room (B_10_10), horizontally and in the middle of the building room (S_55_10), horizontally and near the wall of the building room (B_55_10), on the edge and in the middle of the building room (S_edge), on the edge and near the wall of the building room (B_edge);

- for thermal tests: vertically and in the middle of the building room (S_4), vertically and near the wall of the building room (B_4), horizontally and in the middle of the building room (S_10), horizontally and near the wall of the building room (B_10), on the edge and in the middle of the building room (S_edge), on the edge and near the wall of the building room (B_edge);

- for Shore-D-hardness tests: vertically and in the middle of the building room (S_6), vertically and near the wall of the building room (B_6), horizontally and in the middle of the building room (S_35), horizontally and near the wall of the building room (B_35), on the edge and in the middle of the building room (S_edge), on the edge and near the wall of the building room (B_edge).

After words single virtual models were saved as one file "pack", which was then in RP Tools® divided into layers of predetermined thickness. After parameters of the sintering process were set, a file SLI was created and in PSW® jobfile was prepared and sent as task to Formiga P100. This methodology was shown in Figure 1a. After the sintering was complete, the test specimens were removed from the

building room, cleaned using compressed air, soaked in water to obtain full strength properties, and then measured.
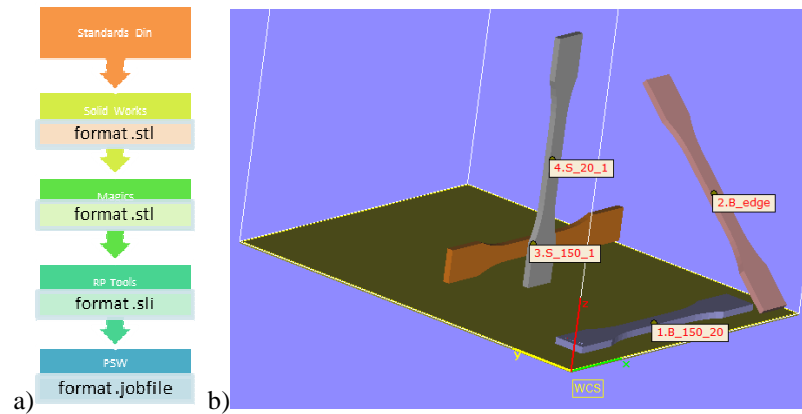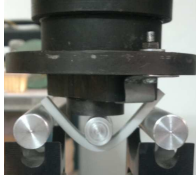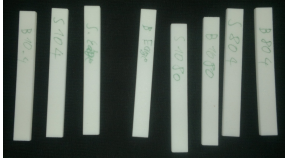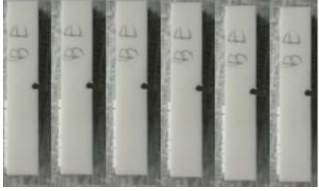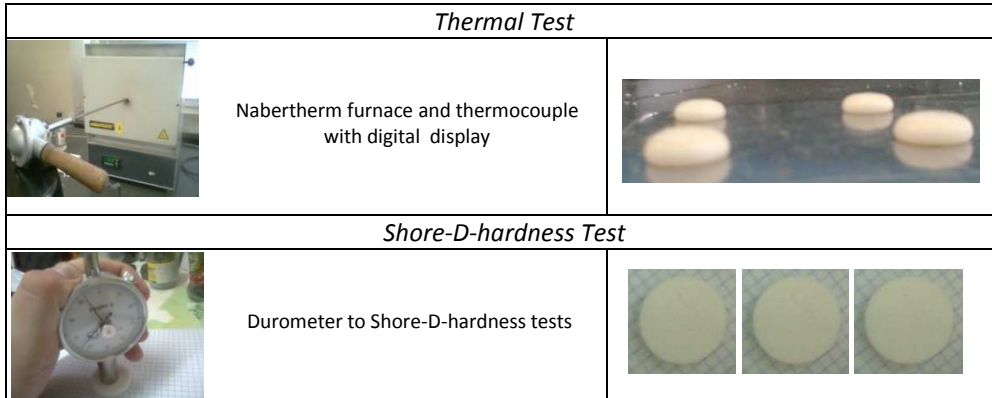

Fig. 1. Methods of preparing the material model building process using SLS technology (a) setting virtual simulation of specimens in the working device SLS - Formiga P100 (b)

Tab. 3. Preparation of thermal and strength tests - material and method

Methods	Material
Strain Test	
Specimen in jaws of Strain Machine Instron 1115	
Bending Test	
The support shafts together with the specimen (left), maximum deflection of the specimen (right)	
Charpy Impact Test	
Charpy Testing Unit	

Thermal Test		
	Nabertherm furnace and thermocouple with digital display	
Shore-D-hardness Test		
	Durometer to Shore-D-hardness tests	

3. Results

3.1 Ultimate tensile strength (UTS)

For the strength tests was used a laboratory stand consisting of Instron 1115 machine and a computer with software that allows to read and analyse the results. There were 8 specimens (made according to DIN EN ISO 527) tested. The extensometer was removed, when the force plot versus the relative elongation stabilized.

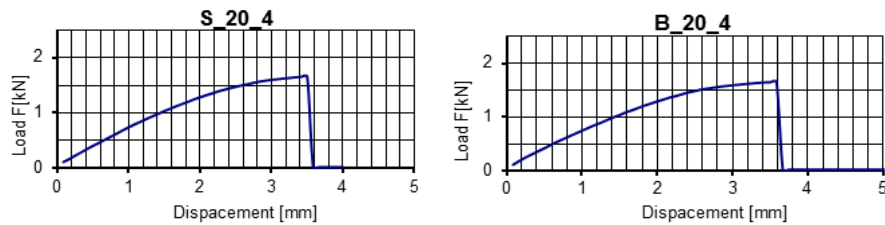The results as the plots of the force versus absolute elongation were shown in Fig. 2-5.

Fig. 2. Plots of force v. elongation for specimens: S_20_1 (left), B_20_1 (right)
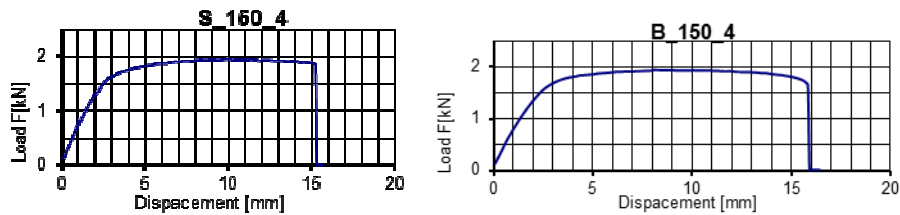

Fig. 3. Plots of force v. elongation for specimens: S_150_4 (left), B_150_4 (right)
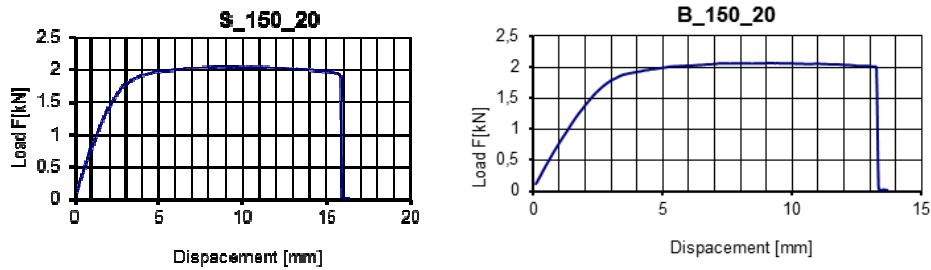
Fig. 4. Plots of force v. elongation for specimens: S_150_20 (left), B_150_20 (right)
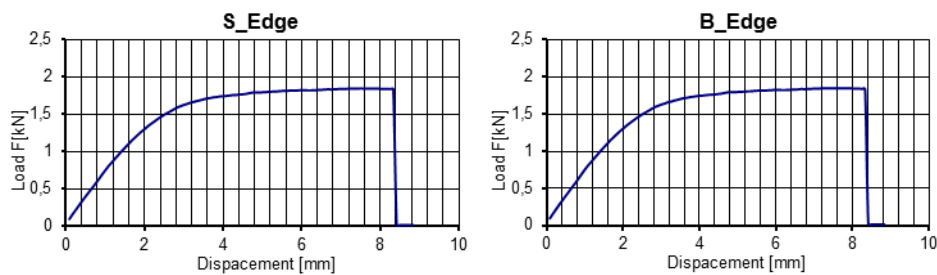

Fig. 5. Plots of force v. elongation for specimens: S_Edge (left), B_Edge (right)

In Table 4 the values of the maximum forces and stresses in the specimen obtained on the uniaxial tensile machine INSTRON and the results of numerical simulations for the solid, injected material (nylon 6) are summarized and compared.

Table 4. Comparison of the results of uniaxial tensile tests for sintered specimens at different orientations and positions with the results of numerical simulations for solid material

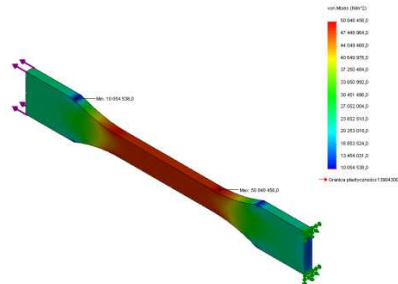| Specimen	Force at break [N]	Tensile strength [MPa] – results of tests	Stress [MPa] – results of simulations
B_20_1	1652	33,40	50,25 MPa
B_150_1	1943	38,86	65,25MPa
B_150_20	2067	41,34	71,09 MPa
B_Edge	1850	37,00	63,70MPa
S_20_1	1653	33,06	50,85 MPa
S_150_1	1953	39,06	66,83MPa
S_150_20	2057	41,14	70,35MPa
S_Edge	1850	37,00	63,70MPa

Fig. 6. Map of reduced stresses von Mises to: F_{max}=1653N; σ_{zred}=50,85 MPa for Nylon 6 (solid material)

3.2 Bending test

The test was conducted on Instron 1115 after changing of the handles. Specimens were placed on two shafts on flank. Every specimen was pressed and deflected by the third shaft. In two cases (specimens: S_10_4 and B_10_4), deflection of the specimen caused breakage. Dependence of the force on deflection is illustrated in Fig. 7-10.
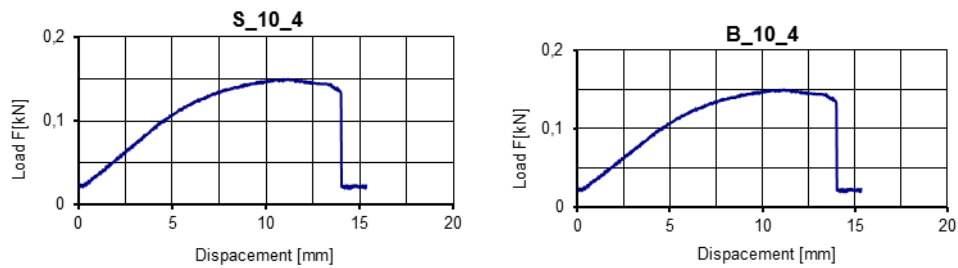

Fig. 7. Plots of force v. deflection for specimens S_10_4 and B_10_4
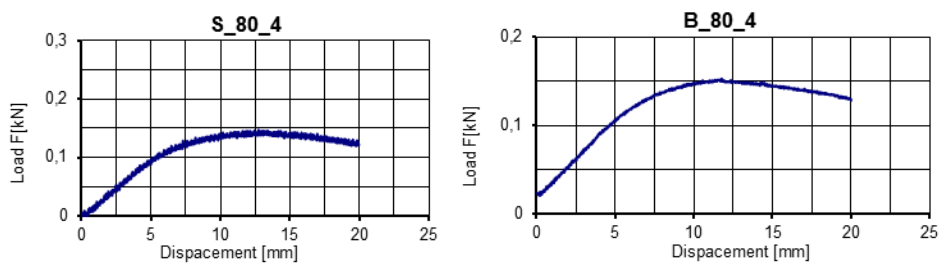

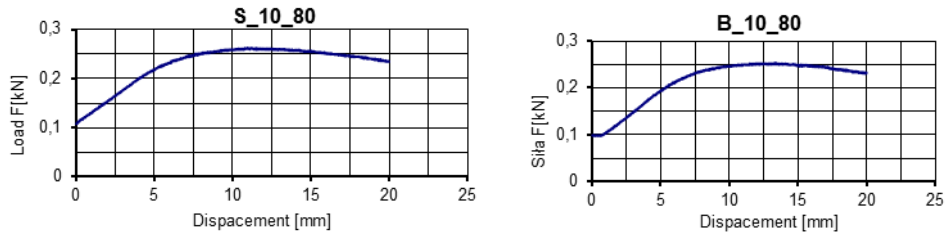Fig. 8. Plots of force v. deflection for specimens S_80_4 and B_80_4

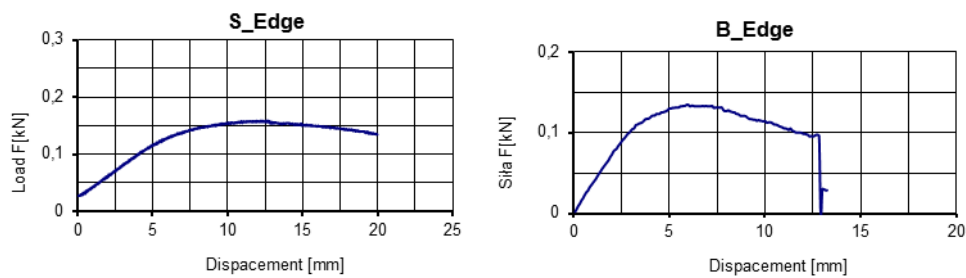Fig. 9. Plots of force v. deflection for specimens S_10_80 and B_10_80

Fig. 10. Plots of force v. deflection for specimens S_Edge and B_Edge

Table 5. Results of bending tests for sintered specimens
at different orientations and positions

Specimens	Maximum force [kN]
B_10_4	0,1493
B_10_80	0,2407
B_80_4	0,1433
B_Edge	0,1347
S_10_80	0,2547
S_80_4	0,1433
S_Edge	0,1540

3.3 Charpy Impact Test

3D geometrical models of notched specimens were made according to DIN EN ISO 179 (Table 1). They were prepared in selective laser sintering process for 6 different positions and orientations. Next they were tested on Charpy-impact unit. The results of these tests are summarized in Table 6.

Tab. 6. Results of Charpy impact tests

Specimens	Energy to break test specimen [kmp]	Value of energy [J]
S_10_10	0,040	0,3923
S_10_55	0,045	0,4413
S_Edge	0,029	0,2844
B_Edge	0,032	0,3138
B_10_10	0,040	0,3923
B_10_55	0,047	0,4609

3.4 Thermal test

Geometrical models of the thermal test specimens were made according to DIN 53736 in 6 copies. A laboratory stand composed of Nabertherm furnace, thermocouple, and a digital display was used to assess the effect of a temperature gradient on the dimensions and structure of the sintered polyamide powder. The aim of the study was to define the temperature in which the specimen gets plasticized. When the temperature exceeded 180°C deflection of specimens was recorded, but they did not change its shape noticeably. Specimens material was plasticizing strongly after exceeding 187°C. The edges were rounded (look at the picture in the Table 3). After cooling, the characteristic dimensions and mass of the specimens were measured and they were compared to the nominal dimensions. Based on these observations it can be concluded that the plastic flow of specimens is regular.

Tab. 7. Results of thermal tests

Specimens	Diameter [mm]	Thickness [mm]	Mass [g]
Nominal size	*10*	*4*	*3,14*
B_10	11,01/10,79	3,98	3,11
S_10	11,05/10,92	4,00	3,12
S_4	10,74/10,68	3,90	2,91
B_4	10,69/10,88	3,82	2,92
S_EDGE	10,74/10,83	3,97	2,91
B_EDGE	10,69/10,88	3,97	3,03

3.5 Shore-D-hardness tests

Specimens for tests of the hardness were made according to DIN 53505. The hardness measurements were made manually with a durometer HBD-100-0. A conical indenter was pressed in the material perpendicular to the specimen surface using c.a. 50N force. The measurement was repeated 10 fold for each of six specimens (Table 8).

Tab. 8. Results of Shore-D-hardness tests

Specimens	S_6	B_6	S_35	B_35	S_Edge	B_Edge
	[HD]	[HD]	[HD]	[HD]	[HD]	[HD]
Measure 1	83	83	81	82	83	83
Measure 2	84	82	82	82	83	82
Measure 3	84	82	82	82	83	82
Measure 4	83	82	81	81	83	82
Measure 5	83	83	82	81	82	82
Measure 6	84	82	81	82	84	83
Measure 7	83	83	81	82	83	83
Measure 8	84	82	82	82	83	82
Measure 9	84	82	82	82	83	82
Measure 10	83	82	81	81	83	82
Average	*83,5*	*82,25*	*81,50*	*81,75*	*83,00*	*82,25*

3.6 Microscopic studies - SEM analysis

A SEM analysis was conducted for a fracture area of 6 specimens, which were tested on Charpy unit previously (S_10_10, B_10_10, S_Edge, B_Edge, S_10_55, B_10_55). The studies were made at the Institute of High Pressures (PAN) with the use of a scanning microscope Zeiss Ultra Plus. This microscope is equipped with 2 detectors of secondary electrons (SE2 and InLens) and two detectors of back-scattered electrons (ESB detector and AsB detector).

Preparation of test specimens consisted of: cutting them to specific dimensions, purging of any impurities using a pneumatic compressor and sprinkling with carbon powder (to perform measurement of the surface structure). Selected photos from the SEM analysis were shown in Fig.s 12-17.
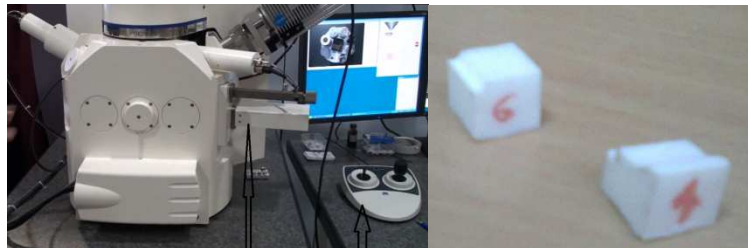

Fig. 11. Analysis of the structure of specimens on the fracture area using scanning electron microscope: microscope Zeiss Ultra Plus (left), specimens (right)
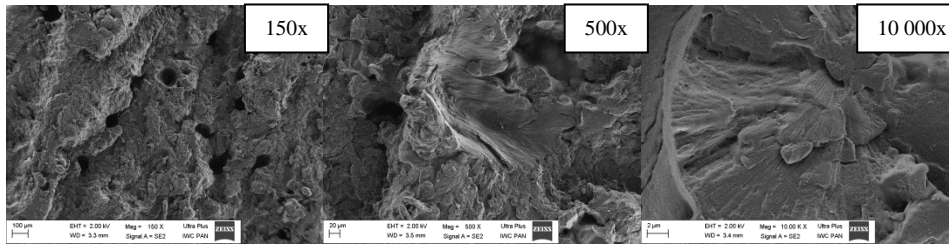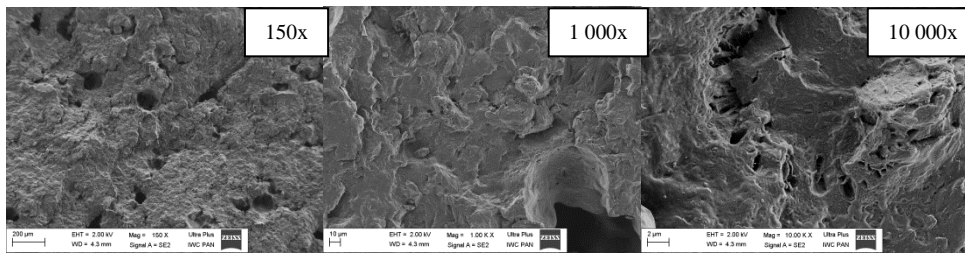
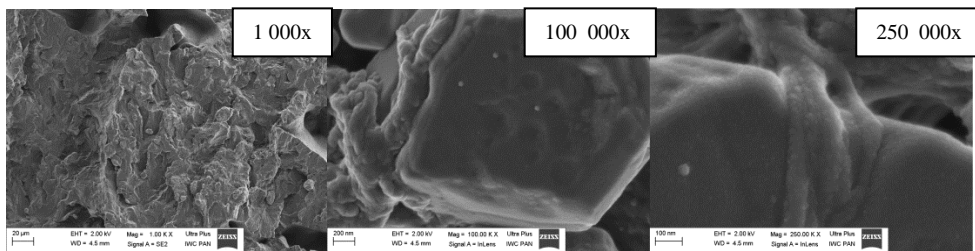Fig. 12. Specimen S10_10
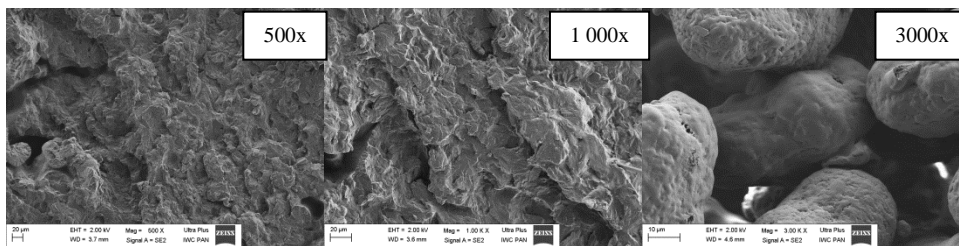

Fig. 13. Specimen B10_10
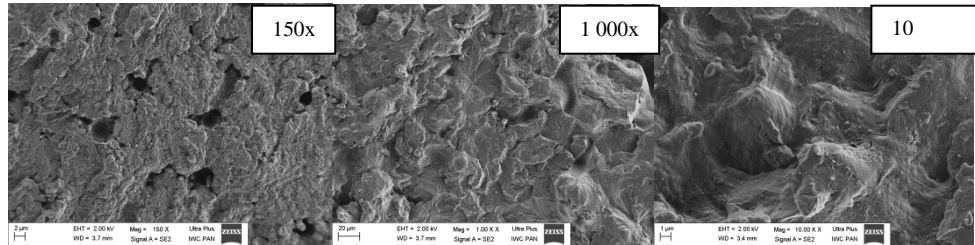

Fig. 14. Specimen S10_55
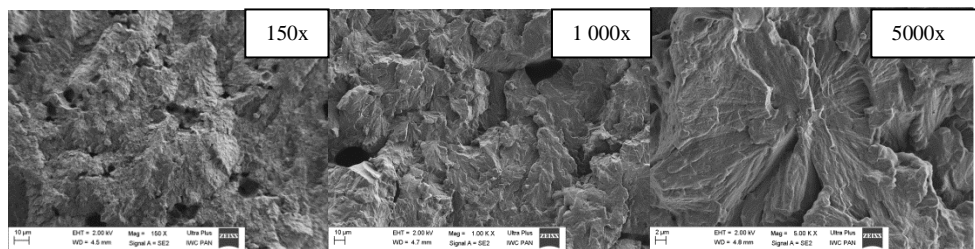

Fig. 15. Specimen B10_55

Fig. 16. Specimen S_Edge

Fig. 17. Specimen B_Edge

4. Discussion and conclusions

On the basis of experimental observations made on sintered specimens of polyamide powders, some conclusions about the impact of the built-orientation in the SLS process on their mechanical, thermal and structural properties can be formulated.

The results (values of the parameters defining the mechanical, thermal and structural properties of components manufactured from polyamide powder) are in line with the observations made by other investigators [Meagan R., et al. 2011, Starr T.L., et al. 2011, Usher J.S., et al. 2001] and the manufacturer of the powder. The impact of the position in the building room (on flank or in the centre) had a negligible effect on the strength of the specimens (up to a few percent). In the case of uniaxial tensile tests (UTS) the specimens built near the wall of the building room were stronger than those in the middle. However, the specimens located in the centre had the best flexural modulus. Charpy tests did not resolve, which of these positions is a better solution, because the specimens built near the wall, with the same geometrical dimensions, had respectively: equal, smaller and larger strength than those in the middle of the building room. In contrast, the specimens which were located on the edge had the best dimensional accuracy in the manufacturer's suggestions. The higher strength of the specimens built at the largest cross-section (horizontal) can be caused by the fact that these specimens have fewer superimposed layers and therefore there are fewer bonds between the layers, whose strength is smaller than that of the layers.

The greatest difference between the specimens' properties in percentage value is: for tension - 20%, for bending - 43.7% and for impact Charpy test - 38.3%. It is worth noting that in the bend test only two weakest specimens were broken (S_10_4 and B_10_4). The results of the strength tests indicate that the horizontal orientation gives the specimens the best dimensional accuracy and the highest mechanical properties. Thermal studies have confirmed melting point for sintered PA2200, stated by the manufacturer. At the higher temperature the specimen starts to plastic flow and changes the profile of surface from rough to smooth. It can be concluded, based on the measurements realized after removing specimens from the furnace that, the orientation and localisation of the specimens do not have any impact on the thermal properties of sintered polyamide powder. The hardness of the specimens is a little higher than nominal. However, a more important conclusion is that the hardness of the material are not linked to the orientation of specimens and their localisation. The microscopic studies have shown that in the Charpy test initially the material gains plasticity and then its rupture. On the picture of specimen B10_55 (Fig. 15) was shown the primary profile of the surface outside a fracture area. The image shows morphology of the surface of the specimen of sintered polyamide located horizontally, near the wall of the building room. There can be seen its granular texture and grain connections.

Therefore it can be concluded that the localisation and orientation of the specimens in the building room have no impact on the thermal and mechanical properties and microstructure or hardness of polyamide powder. Thus the results should encourage the use of selective laser sintering technique in large-scale manufacturing. The essential differences are present in the mechanical properties – the most durable were the horizontally built specimens and the weakest – those built vertically.

It failed to observe a correlation between the location of the specimens in the building room of the device (middle/flank) and mechanical properties. Probably, the effect associated with the impact of part position and correlated with it the gradient of temperature on the mechanical properties is negligible for small elements such as the test specimens.

References

Ajoku, U., Saleh, N., Hopkinson, N., Hague, R.J.M. and Erasenthiran P., 2006, Investigating mechanical anisotropy and end-of-vector effect in laser-sintered nylon parts, Proceedings of the Institution of Mechanical Engineers Part B – Journal of Engineering Manufacture, vol. 220, no. 7, p. 1077-1086.

Anitha R., Arunachalam S., Radhakrishnan P., 2001, Critical parameters influencing the quality of prototypes in fused deposition modeling, Journal of Materials Processing Technology, vol. 118, 2001, p. 385-388

Caulfield, B., McHugh, P.E. and Lohfeld, S., 2007, Dependence of mechanical properties of polyamide components on build parameters in the SLS process, Journal of MaterialsProcessingTechnology,vol.182, No 1, 2007, p. 477-488

Cheng W., Fuh J.Y.H., Nee A.Y.C., Wong Y.S., Loh H.T., Miyazawa T., 1995, Multi-objective optimization of part-building orientation in stereolithography, Rapid Prototyping Journal, vol. 1, nr 4, 1995, p. 12-23

Choren, J., Gervasi, V., Herman, T., Kamara, S. andMitchell, J., 2001, SLS powder life study, paper presented at Twelfth Annual International Solid FreeformFabrication Symposium, University of Texas at Austin, 2001, Austin, TX.

Dąbrowska-Tkaczyk A., Floriańczyk A., Grygoruk R., Skalski K., Borkowski P., 2011, Virtual and material models of human thoracic-lumbar spine with compressive fracture based on patients' CT data and the Rapid Prototyping Technique, The Archive of Mechanical Engineering, vol. LVIII, 2011, nr 4, p. 429-439

Dingal S., Pradhan T. R., Sarin Sundar J. K., Roy Choudhury A., Roy S. K., 2008, The application of Taguchi's method in the experimental investigation of the laser sintering process, Int J Adv Manuf Technol (2008) 38:904–914

Gibson I., Stucker B., Rosen D., 2009, Additive Manufacturing Technologies: Rapid Prototyping to Direct Digital Manufacturing, Springer, 2009

Jhabvala J., Boillat E., Glardon R., 2013, Study of the inter-particle necks in selective laser sintering, Rapid Prototyping Journal, vol. 19, nr 2, 2013, p. 111-117

Mager A., Moryson G., Cellary A., Marciniak M., 2011, Zastosowanie technik rapid prototyping do wytwarzania wyrobów metalowych, Postępy Nauki i Techniki, 2011, 8, p. 174-182

Majewski, C., Zarringhalam, H. and Hopkinson, N., 2008, Effect of the degree of particle melt on mechanical properties in selective laser-sintered nylon-12 parts, Proceedings of the Institution of Mechanical Engineers Part B – Journal of Engineering Manufacture, vol. 222, no. 9, 2008, p. 1055-1064

Meagan R. Vaughan M.R., Crawford R.H., 2011, Effectiveness of virtual models in design for additive manufacturing: a laser sintering case study, Rapid Prototyping Journal, vol. 19, nr 1, 2013, str. 11-19 Nikzad M., Masood S.H., Sbarski I., Thermo-mechanical properties of a highly filled polymeric composites for Fused Deposition Modeling, Materials and Design, vol. 32, 2011, p. 3448

Parthasarathy J., Starly B., Raman S., 2011, A design for the additive manufacture of functionally graded porous structures with tailored mechanical properties for biomedical applications, Journal of Manufacturing Processes, vol. 13, 2011, p. 160–170

Ramos-Grez, J., Amado-Becker, A., Yan˜ ez, M.J., Vargas, Y. and Gaete, L., 2008, Elastic tensor stiffness coefficients for SLS nylon 12 under different degrees of densification as measured by ultrasonic technique, Rapid Prototyping Journal, vol. 14 no. 5, 2008, p. 260-270

Singh R., 2013, Some investigations for small-sized product fabrication with FDM for plastic components, Rapid Prototyping Journal, 2013, vol. 19, no 1, 2013, p. 58-63

Starr, T.L., Gornet, T.J. and Usher, J.S., 2011, The effect of process conditions on mechanical properties of laser sintered nylon, Rapid Prototyping Journal, Vol. 17 No. 6, 2011

Usher J.S., Gornet T.J., Starr T.L., 2013, Weibull Growth Modeling of Laser-Sintered Nylon 12, Rapid Prototyping Journal, vol. 19, nr 4, 2013, p. 301-306

Usher, J.S. and Srinivasan, M.K., 2001, Quality improvement of a selective laser sintering process, Quality Engineering, vol. 13 no. 2, 2001, p. 161-168

Vandenbroucke B., Kruth J-P., 2007, Selective laser melting of biocompatible metals for rapid manufacturing of medical parts, Rapid Prototyping Journal, vol. 13, nr 4, 2007, p. 196-203

Wesley M., Cunico M., de Carvalho J., Optimization of positioning system of FDM machine design using analytical approach, Rapid Prototyping Journal, vol. 19, nr 3, 2013, p. 144-152

Zarringhalam, H., Hopkinson, N., Kampermanb, N.F. and Vlieger, J.J.de , 2013, Effects of processing on microstructure and properties of SLS nylon 12, Materials Science & Engineering A: Structural Materials Properties Microstructure and Processing, vol. 435, 2006, p. 172-180

Standards: DIN EN ISO 527, DIN EN ISO 178, DIN EN ISO 179, DIN 53505, DIN 53736

www.eos.info [2013]